

# A modified CPS-PWM for capacitor voltage reduction of MMC based variable speed drive

Safia Babikir Bashir<sup>1</sup>, Hasan Abdel Rahim A. Zidan<sup>2</sup>, Zulfiqar Ali Memon<sup>2</sup>

<sup>1</sup>Research Institute of Science and Engineering, University of Sharjah, Sharjah, United Arab Emirates

<sup>2</sup>Electrical and Computer Engineering Department, College of Engineering, Ajman University, Ajman, United Arab Emirates

## Article Info

### Article history:

Received Apr 2, 2022

Revised May 28, 2022

Accepted Jun 20, 2022

### Keywords:

CPS-PWM

MMC

SM voltage ripples

Variable speed drive

## ABSTRACT

In recent years, modular multilevel converters (MMC) have become one of the most popular multilevel converter topologies. Despite its growing popularity, MMC is still less widespread in variable speed drives (VSDs) applications. The reason for this is that the voltage ripple of the MMC submodules (SM) increases during the low-speed constant torque operation. In this paper, carrier phase shift-pulse width modulation (CPS-PWM) is modified to reduce the average voltage of SM and thus accommodate more ripples without exceeding the maximum SM voltage. The proposed method does not involve the injection of circulating current components, thereby resulting in less power loss. In addition to that, the necessity for increasing the SM capacitor rating during low-speed operation is not required. Extensive simulation has been conducted under various speed commands to validate the effectiveness of this method.

*This is an open access article under the [CC BY-SA](https://creativecommons.org/licenses/by-sa/4.0/) license.*



## Corresponding Author:

Safia Babikir Bashir

Research Institute of Science and Engineering, University of Sharjah

Sharjah, United Arab Emirates

Email: safia.mohamed@sharjah.ac.ae

## 1. INTRODUCTION

Nowadays, multilevel converters are gaining more popularity in industrial applications. This is attributed to the increased demand for high power and voltage in these applications. The multilevel converters offer several advantages over traditional two-level converters such as high power and high output voltage levels capability, reduced filtering requirement, and reduced electromagnetic interferences [1], [2]. The available multilevel converters topologies are neutral-point-clamped (NPC) converters [3], flying capacitor (FC) converters [4], cascaded h-bridge (CHB) converters [5], and modular multilevel converters (MMC). The MMC is relatively the newest multilevel converter that was developed by Lesnicar and Marquardt in 2003 [6].

Among the above mentioned multilevel converters, the MMC offers additional features [7], [8]. Scalability and modularity are some of these unique features that facilitate the extension of the voltage level and power rating by simply increasing the number of submodules (SM). Reliability can be improved easily in this topology by introducing additional SM, that will be switched ON in case of SM failure. In addition, the MMC can offer a transformer-less operation.

Despite all these features, the use of MMC in VSD applications is still limited. The reason behind this limited usage is that the voltage ripples of SMs are directly proportional to the amplitude of output current and inversely proportional to its frequency, thus during low-speed constant torque operation of VSD the voltage ripples of SM increases [9]. Therefore, to compensate for the large capacitor voltage ripples when operating at low-speed constant torque, the rated value of the SMs capacitor must be increased [2].

To overcome the problem of the increased voltage ripples lot of research has been conducted in recent years. Korn *et al.* [9], proposed injecting high frequency components into the circulating current to reduce the fundamental ripples of SMs. Picas *et al.* [10] developed the injection of second-order harmonic component into the circulating current. In addition to the second harmonic injection [11] and [12] proposed the injection of the fourth harmonic in the circulating current. The main drawback of these proposed injection methods is that they increase the power losses as well as overrating the power devices in the MMC topology [13]. Apart from this, all these injection methods use lookup table to calculate the required injected values of the circulating current [14]. The research work in [15] provides real-time calculations of the injected circulating current. However, these calculations ignore the power losses [16]. Most of the above-mentioned proposed method injects a common-mode voltage along with the circulating current component as in [9], [17].

The common-mode voltage appears on the motor winding and result in a current flowing through the bearing, which may cause permanent failure. In [18], [19], it was reported that the DC bus voltage could be reduced by using another MMC as an active front end (AFE) rectifier in order to reduce the SM voltage ripples. Using an AFE rectifier is practical when the regenerative mode is needed. However, when the regenerative mode is not needed, the additional MMC increases the system costs.

The work [2] adds an active power filter (APF) to each SM in order to reduce the SM capacitor voltage. Despite the reduction of SM voltage ripples, it requires twice the number of IGBTs and capacitors compared to the conventional MMC. The work [20] proposes a modified MMC with an (APF) that connects this filter between the last SM in the upper arm and the first SM in the lower arm to divert the power ripples into the capacitor of the APF. However, this modified topology also increases the number of IGBTs and capacitors. Moreover, the SM balancing method is slow when the number of SMs is large.

Another proposed solution to the problem of increased SM capacitors voltage ripples is to reduce the average voltage of the SM during low-speed constant torque operation as proposed in [21]. However, finding the optimal average voltage increases the computation burden. Moreover, this method will not be effective at speeds that are less than one-third of the rated speed.

In this paper an approach for reducing the SM average voltage during low-speed constant torque operation is proposed. It was observed that during low-speed operation the number of SMs inserted in each arm decreases with the reduction of reference voltage. Therefore, the CPS-PWM is modified in this paper in such a way that each arm has one more SM inserted. Thus, two more SMs are inserted into each phase, which will result in a reduction of the SM voltage. As a result, higher capacitor voltage ripples can be tolerated without crossing the capacitor voltage limit. This is the main contribution of this paper. The merit of using this method is the elimination of the need for overrating SM capacitors. Moreover, it does not require the injection of an oscillating component in the circulating current and the common-mode voltage that is widely used to reduce the capacitor voltage ripples. Therefore, no additional losses are created.

This paper is organized as follows, the MMC basic structure and operation principle are presented in section 2. The explanation of the proposed Modified CPS-PWM is given in section 3. Section 4 tests the effectiveness of the proposed method. Finally, the concluding remarks are given in section 5.

## 2. MODULAR MULTILEVEL CONVERTER

### 2.1. Basic structure and operation principle

The development of the modular multilevel converter in 2003 by Lesnicar and Marquardt is considered a breakthrough in multilevel converter topology. Figure 1(a) shows the basic circuit structure of MMC. Each phase in the MMC is divided into two arms and each arm consists of N submodules that are connected in series. The SM configuration that is used in this paper is the half-bridge circuit and it basically consists of a capacitor and active switching devices as depicted in Figure 1(b). When the upper switch is on, and the lower switch is off the SM is inserted in the arm circuit and the SM voltage is equal to the capacitor voltage. In contrast, the SM is bypassed when the lower switch is on, and the upper switch is off resulting in zero SM voltage. A staircase voltage is formed at the MMC output terminals by varying the number of bypassed and inserted SMs.

### 2.2. Mathematical model of MMC

For the purpose of simplifying the development of the MMC mathematical model, the SMs of the upper and the lower arms are replaced by a voltage source ( $v_u, v_l$ ) as shown in Figure 2. The relationship between the arm voltages DC link voltage, and the output voltages are obtained by applying Kirchhoff's voltage law as follow:

$$\frac{v_{dc}}{2} - v_o = v_u + Ri_u + L \frac{di_u}{dt} \quad (1)$$

$$\frac{v_{dc}}{2} + v_o = v_l + Ri_l + L \frac{di_l}{dt} \tag{2}$$

$$i_o = i_u - i_l \tag{3}$$

where  $i_u$  and  $i_l$  are the currents in the upper and lower arms, respectively. The equivalent resistance of the semiconductor switches and cables is represented by  $R$ , While arm inductance is denoted by  $L$ ,  $v_o$  and  $i_o$  are the output voltage and current, respectively.

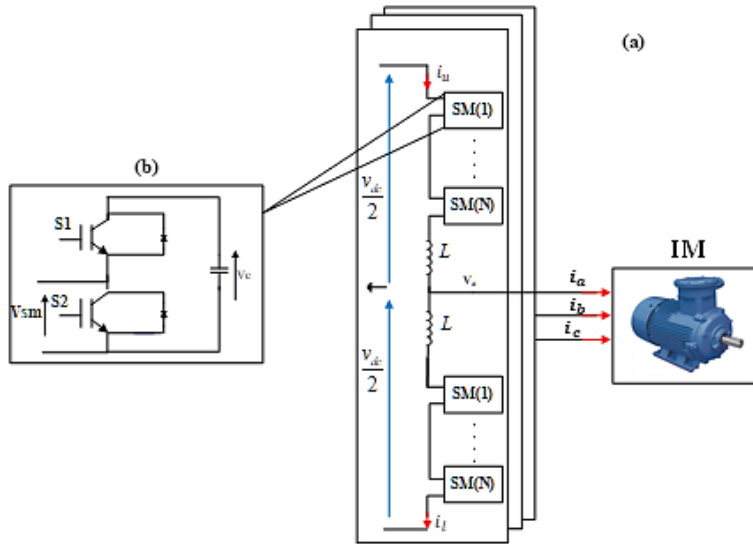


Figure 1. Three-phase MMC based VSD: (a) MMC and (b) SM

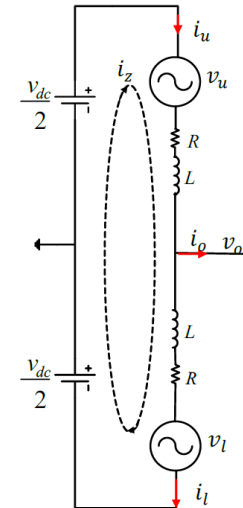


Figure 2. Single phase MMC

The arm currents are represented by (4).

$$i_u = \frac{i_o}{2} + i_z, i_l = -\frac{i_o}{2} + i_z \tag{4}$$

Where  $i_z$  represent the circulating current that goes inside the MMC, and it is given by (5).

$$i_z = \frac{i_u + i_l}{2} \tag{5}$$

Subtracting (1) from (2) and substituting  $i_o$  for  $i_u - i_l$  the following in (6).

$$\frac{v_l - v_u}{2} = v_o + \frac{R}{2}i_o + \frac{L}{2} \frac{di_o}{dt} \tag{6}$$

The term  $(v_l - v_u)/2$  in (6) represent the inner emf voltage that yields the MMC output current and for simplicity, it is replaced by  $e_j$  as (7).

$$e_j = v_o + \frac{R}{2}i_o + \frac{L}{2} \frac{di_o}{dt} \tag{7}$$

Adding (2) to (1) and by substituting  $(i_u + i_l)/2$  by  $i_z$  in (8).

$$L \frac{di_z}{dt} + Ri_z = \frac{V_{dc}}{2} - \frac{v_u + v_l}{2} \tag{8}$$

By substituting the term  $(V_{dc}/2) - (v_u + v_l)/2$  by  $v_z$  in (9).

$$L \frac{di_z}{dt} + Ri_z = v_z \tag{9}$$

Where  $v_z$  is the voltage that produces the circulating current inside the MMC. From the above equations, the upper and the lower arm voltage are givens as follows:

$$\begin{aligned} v_u &= \frac{V_{dc}}{2} - e_j - v_z \\ v_l &= \frac{V_{dc}}{2} + e_j - v_z \end{aligned} \quad (10)$$

### 2.3. MMC during low-speed constant torque operation

As stated previously in the introduction, MMC is still not widely used for VSD applications due to the increased voltage ripple caused by constant torque low-speed operation. To understand the reasons behind this increased voltage ripples, consider the following equations.

The upper and lower arm powers in each phase are given as:

$$P_{xu} = v_{xu} i_{xu} = \left( \frac{V_{dc}}{2} - e_j \right) \left( \frac{i_o}{2} + i_z \right) \quad (11)$$

$$P_{xl} = v_{xl} i_{xl} = \left( \frac{V_{dc}}{2} + e_j \right) \left( -\frac{i_o}{2} + i_z \right) \quad (12)$$

to simplify the analysis in these equations, the voltage drop across the arm inductor and resistor are neglected, therefore the emf voltage in (7) will be equal to the MMC output voltage ( $e_j = v_o$ ). Thus, (11) and (12) becomes:

$$P_{xu} = v_{xu} i_{xu} = \left( \frac{V_{dc}}{2} - v_o \right) \left( \frac{i_o}{2} + i_z \right) \quad (13)$$

$$P_{xl} = v_{xl} i_{xl} = \left( \frac{V_{dc}}{2} + v_o \right) \left( -\frac{i_o}{2} + i_z \right) \quad (14)$$

The MMC output voltage and current are represented by:

$$v_o = V_o \cos \omega t \quad (15)$$

$$i_o = I_o \cos (\omega t - \varphi) \quad (16)$$

where  $V_o$  and  $I_o$  are the output voltage and the output current magnitude respectively,  $\omega$  is the angular frequency of the output and  $\varphi$  is the phase lag angle.

In this paper the circulating current  $i_z$  harmonic components are suppressed only if-else is stated. Therefore, the circulating current consists only of a DC component that ensures the power balance between the DC and AC sides. Thus, according to [13] the circulating current is given by (17).

$$i_z = \frac{1}{4} m I_o \cos \varphi \quad (17)$$

Where  $m$  is the modulation index and it relates the MMC output voltage and DC voltage by (18).

$$m = \frac{2V_o}{V_{dc}} \quad (18)$$

Substituting (15)-(18) into (13) and (14) and rearranging the equations:

$$P_{xu} = \frac{V_{dc} I_o}{4} \left[ \cos (\omega t - \varphi) - \frac{m^2}{2} \cos (\omega t) \cos (\varphi) - \frac{m}{2} \cos (2\omega t - \varphi) \right] \quad (19)$$

$$P_{xl} = \frac{V_{dc} I_o}{4} \left[ -\cos (\omega t - \varphi) + \frac{m^2}{2} \cos (\omega t) \cos (\varphi) - \frac{m}{2} \cos (2\omega t - \varphi) \right] \quad (20)$$

The upper and the lower arm energy are obtained by integrating (19) and (20).

$$E_{xu} = \frac{V_{dc} I_o}{4} \left[ \frac{1}{\omega} \sin (\omega t - \varphi) - \frac{m^2 \cos (\varphi)}{2\omega} \sin \omega t - \frac{m}{4\omega} \sin (2\omega t - \varphi) \right] \quad (21)$$

$$E_{xl} = \frac{V_{dc} I_o}{4} \left[ -\frac{1}{\omega} \sin (\omega t - \varphi) + \frac{m^2 \cos (\varphi)}{2\omega} \sin \omega t - \frac{m}{4\omega} \sin (2\omega t - \varphi) \right] \quad (22)$$

When it comes to VSD application, the term  $m/\omega$  is constant, therefore the third term on the right-hand side of (21) and (22) is constant. On the other hand, the first term in (21) and (22) will increase with the increase in speed while the second term will decrease. During low-speed operation the dominant term in case of energy variations is the first term, thus (21) and (22) will be:

$$E_{xu} = \frac{V_{dc}I_o}{4} \left[ \frac{1}{\omega} \sin(\omega t - \varphi) \right] \quad (23)$$

$$E_{xl} = \frac{V_{dc}I_o}{4} \left[ -\frac{1}{\omega} \sin(\omega t - \varphi) \right] \quad (24)$$

The peak-to-peak energy variation is given as (25).

$$\Delta E_{xu} = \Delta E_{xl} = \frac{2P_o}{\omega} \quad (25)$$

Where  $P_o = V_{dc}I_o/4$  and is related to the SMs voltage ripples as:

$$\frac{2P_o}{\omega} = N \left( \frac{1}{2} C V_{c(\max)}^2 - \frac{1}{2} C V_{c(\min)}^2 \right) = N V_c C \Delta V_c \quad (26)$$

$\Delta V_c$  is peak to peak capacitor voltage ripple of the SM. The term  $N V_c$  is equal to  $V_{dc}$ . Thus, the SM voltage ripple can be represented as (27).

$$\Delta V_c = \frac{2P_o}{\omega C V_{dc}} = \frac{I_o}{2\omega C} \quad (27)$$

From (27) it is obvious that the voltage ripple of the SM capacitor is directly proportional to the output current magnitude of the MMC and inversely proportional to its frequency. Therefore, during low-speed operation the SM voltage ripples increase drastically.

### 3. MODIFIED CPS-PWM

When low-speed operation is used, the voltage reference from the field oriented control (FOC) is reduced, which will affect the number of SMs inserted into each arm. To understand the reasons behind the reduction of the inserted number of SMs in each arm consider the (28).

$$v_{ref} = m \cos(\omega t) \quad (28)$$

In (28) represents the reference voltage obtained from FOC. This reference voltage is related to the output voltage by (29).

$$v_o = \frac{V_{dc}}{2} v_{ref} = \frac{V_{dc}}{2} m \cos(\omega t) \quad (29)$$

Substituting (29) in the upper and lower arm voltages in (10), recalling that ( $e_j = v_o$ ) and neglecting  $v_z$ , we get

$$v_u = \frac{V_{dc}}{2} - \frac{V_{dc} m \cos(\omega t)}{2} \quad (30)$$

$$v_l = \frac{V_{dc}}{2} + \frac{V_{dc} m \cos(\omega t)}{2} \quad (31)$$

these arm voltages can also be represented by:

$$v_u = n_u \sum v_c \quad (32)$$

$$v_l = n_l \sum v_c \quad (33)$$

in these two equations,  $n_u$  and  $n_l$  represent the upper arm and the lower arm insertion ratios, where  $\sum v_c$  represent the sum of SMs voltages in each arm and it's expressed as (34).

$$\sum v_c = N v_c = N * \frac{v_{dc}}{N} \quad (34)$$

Where  $N$  denotes the total number of available SMs in each arm. The result of substituting (34) in (32) and (33) is:

$$v_u = n_u V_{dc} = \frac{V_{dc}}{2} - \frac{V_{dc} m \cos(\omega t)}{2} \quad (35)$$

$$v_l = n_l V_{dc} = \frac{V_{dc}}{2} + \frac{V_{dc} \cos(\omega t)}{2} \quad (36)$$

each arm's insertion ratio can be determined by rearranging the above equations as follows:

$$n_u = \frac{v_u}{V_{dc}} = \frac{1 - m \cos(\omega t)}{2} = \frac{1}{2} (1 - v_{ref}) \quad (37)$$

$$n_l = \frac{v_l}{V_{dc}} = \frac{1 + m \cos(\omega t)}{2} = \frac{1}{2} (1 + v_{ref}) \quad (38)$$

It is obvious from (37) and (38) that the insertion ratio is directly proportional to the reference voltage. Therefore, during low-speed operation, the insertion ratio is reduced.

In each arm, the number of SM inserted ( $N_u, N_l$ ) is related to the insertion ratio by:

$$N_u = n_u * N \quad (39)$$

$$N_l = n_l * N \quad (40)$$

In this paper, the number of inserted SMs in each arm will be increased by one. As a result, the number of inserted SMs in each arm will vary between (2 to  $N$ ). As a result, in (39) and (40) becomes:

$$N'_u = (n_u * N) + 1 \quad (41)$$

$$N'_l = (n_l * N) + 1 \quad (42)$$

This will result in increasing the total number of inserted SMs in each phase from  $N$  to  $N + 2$  or ( $N - 1, N, N + 1$ ) to ( $N + 1, N + 2, N + 3$ ) depending on the modulation mode. This will lead to the reduction of the SM capacitor voltage from ( $v_c = v_{dc}/N$ ) in (43).

$$v'_c = \frac{V_{dc}}{N+2} \quad (43)$$

By reducing the average SM capacitor voltage more voltage ripples can be accommodated without exceeding the maximum voltage limit. The circulating current control in this paper uses the redundancies states in the  $2N + 1$  modulation mode that was proposed in [22]. The advantage of this approach is that it controls the circulating current directly by selecting the number of SMs within the arm so that the circulating current is driven to its reference. By doing this the requirement of injecting additional voltage reference to the output voltage reference is not needed, which is a big advantage in the VSD application. In general, MMC can generate  $N+1$  or  $2N+1$  voltage levels at the output depending on the modulation mode that is used. The  $2N + 1$  modulation differs from  $N + 1$  modulation by generating additional voltage levels which are intermediate voltage levels to that of the  $N + 1$ . These intermediate voltage levels are the results of inserting ( $N + 1$ ) or bypassing ( $N - 1$ ) SMs in each phase and are known as the redundant states. These two redundant states can be utilized to control the circulating current ( $i_z$ ). The basic idea of this circulating current control method is that if  $i_z$  is higher than the reference circulating current ( $i_z^*$ ) then additional SM will be inserted into each phase ( $N + 1$  state) which will reduce the circulating current. On the other hand, if  $i_z$  is lower than the ( $i_z^*$ ) then a SM will be removed from each phase ( $N-1$  state) to increase the circulating current.

In this paper, this method is modified to reduce the average voltage of SMs during low-speed constant torque and at the same time control the circulating current without injecting additional voltage to the reference voltage. Figure 3 illustrates the proposed method. The reference voltage that is obtained from the FOC is given to the CPSPWM to obtain the level (X). The reference circulating current is compared with the actual circulating current and the result of the comparison (I) is passed to the selection block. The selection block is illustrated in Figure 4 and based on the voltage level (X) and output of the comparison (I), The selection block will decide the number of SMs in each arm ( $N_u, N_l$ ). This number is then increased by one ( $N'_u, N'_l$ ) to reduce the average voltage of SM during low-speed operation. ( $N'_u, N'_l$ ) are then given to the balancing method to determine which SM should be turned on based on the SM voltage level, number of SM, and the direction of the arm current [23]-[25].

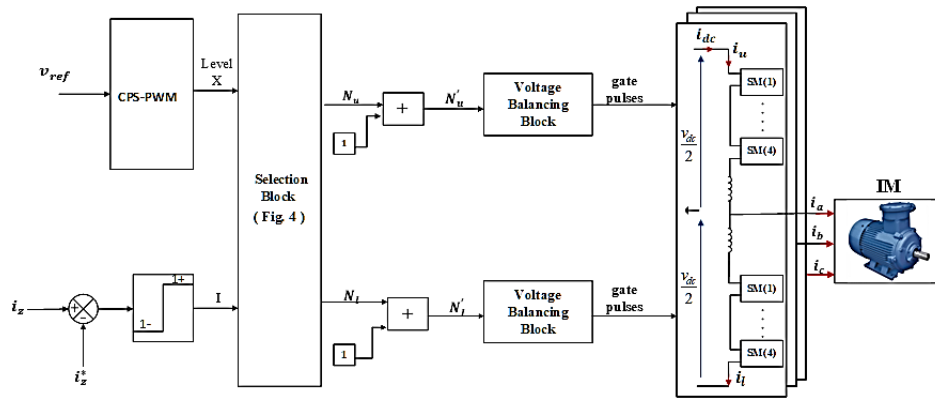


Figure 3. Modified CPS-PWM

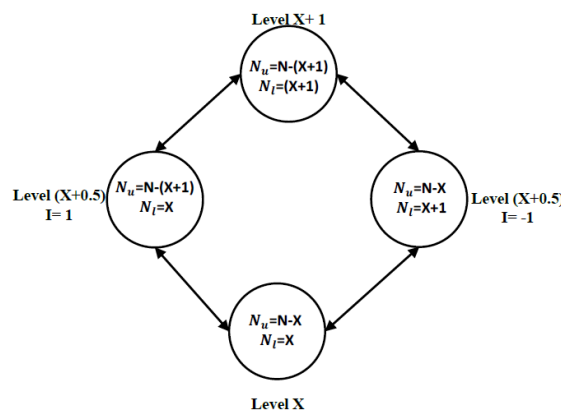


Figure 4. Selection block

**4. SIMULATION RESULTS**

For the purpose of verifying the proposed method, a MATLAB/SIMULINK simulation model of 5-level MMC based VSD was developed. MMC and induction motor parameters are presented in Table 1. The results presented in this section were obtained by operating the MMC at low speeds (1 Hz, 5 Hz, 10 Hz) with constant load torque.

Table 1. System parameters

	Parameter	Value
Inductor motor (IM)	Active power (rated)	$P = 3.75 \text{ KW}$
	Poles pair	$PP = 2$
	Current (rated)	$I = 8.5 \text{ A}$
	IM nominal frequency	$f_0 = 50 \text{ Hz}$
	Start resistance	$R_s = 4.6 \Omega$
	Stator inductance	$L_s = 0.797 \text{ H}$
	Rotor resistance	$R_r = 4.94 \Omega$
	Rotor inductance	$L_r = 0.797 \text{ H}$
	Mutual inductance	$L_m = 0.768 \text{ H}$
	Inertia	$J = 0.03 \text{ Kg.m}^2$
	Torque (rated)	$T_{rated} = 23.87 \text{ N.m}$
MMC	Dc-link voltage	$V_{dc} = 600\text{V}$
	Number of SM	4
	Arm inductance	$L = 1.5\text{m H}$
	Submodule capacitance	$C = 1.2\text{m F}$
	Switching frequency	$f_{sw} = 5\text{KHz}$

**4.1. Case 1: Speed=1 Hz (30 rpm)**

In this case, the MMC based VSD was operating at a very low speed 30 rpm (1 Hz) with a 40% load torque as illustrated in Figure 5. Figure 6 illustrates the SM capacitor voltages of phase a. It is clear from

Figure 6(a) that when the conventional CPS-PWM was used the voltage ripples increased and the maximum voltage has exceeded the maximum capacitor voltage limits (157 V) by 23 V approximately. In contrast, the maximum voltage ripples in the modified CPS-PWM without and with the circulating currents control Figure 6(b) and Figure 6(c) respectively were less than the Maximum capacitor voltage limits (157 V) by 27 V approximately.

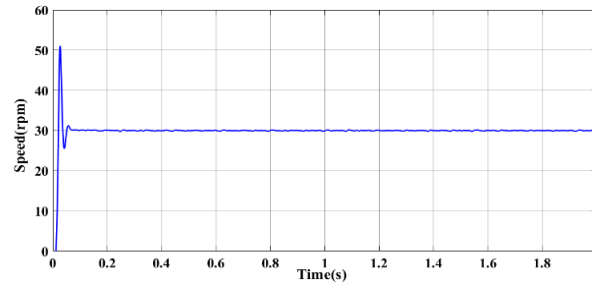


Figure 5. Response of the induction motor to 30 rpm speed command

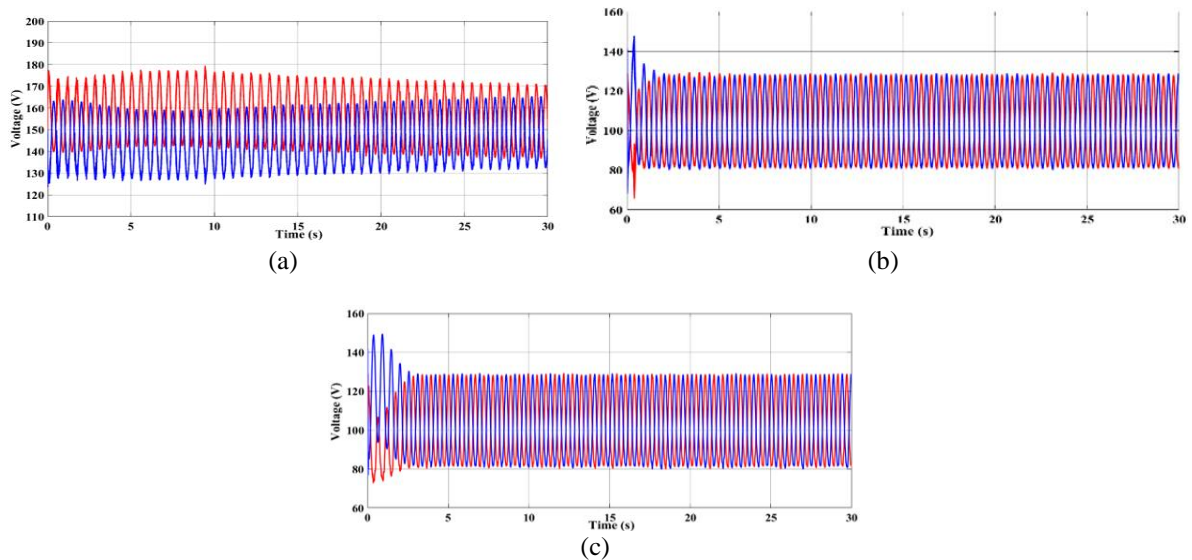


Figure 6. The voltages of SMs capacitors in phase-a (a) conventional CPS-PWM, (b) modified CPS-PWM, and (c) modified-CPS-PWM with circulating current control

Thus, by reducing the SM nominal voltage in the proposed method the requirement of increasing the capacitor rating is not needed. Figures 7(a), 7(b) and 7(c) shows the output currents when the conventional CSP-PWM and the modified CSP-PWM with or without the circulating current control are used. It is clear from Figures 7(a) and 7(b) that the MMC output current is not affected by the proposed method. Figure 8 demonstrates the number of SMs in each phase when the conventional CSP-PWM Figure 8(a) and the modified CSP-PWM (with or without the circulating current control) Figure 8(b) and Figure 8(c) were used. In conventional CSP-PWM, the average number of inserted SMs in each phase is  $4(N=4)$ . On the other hand, when the modified CSP-PWM the number of SMs in each phase is increased by two and as a result, the number of inserted SMs in each phase is  $6(N+2)$ . When the modified CPS-PWM with the circulating current control was used the number of inserted SMs varies between 5.6, and  $7(N+1, N+2, \text{ and } N+3)$ . The advantage of using the modified CPS-PWM with circulating current control is demonstrated in Figure 9. It is obvious that the modified CPS-PWM with circulating current control has resulted in less circulating current compared to the conventional CSP-PWM. The effect of the proposed method on the common-mode voltage (CMV) is given in Figure 10. It is clear that the CMV when the modified CPS-PWM is used was less than the conventional CSP-PWM by approximately 18 V. Figure 11 illustrate the upper arm current of phase-a ( $i_{au}$ ) When the circulating current control is activated, the arm current was reduced in the modified proposed CPS-PWM, which will result in less power loss in the MMC.

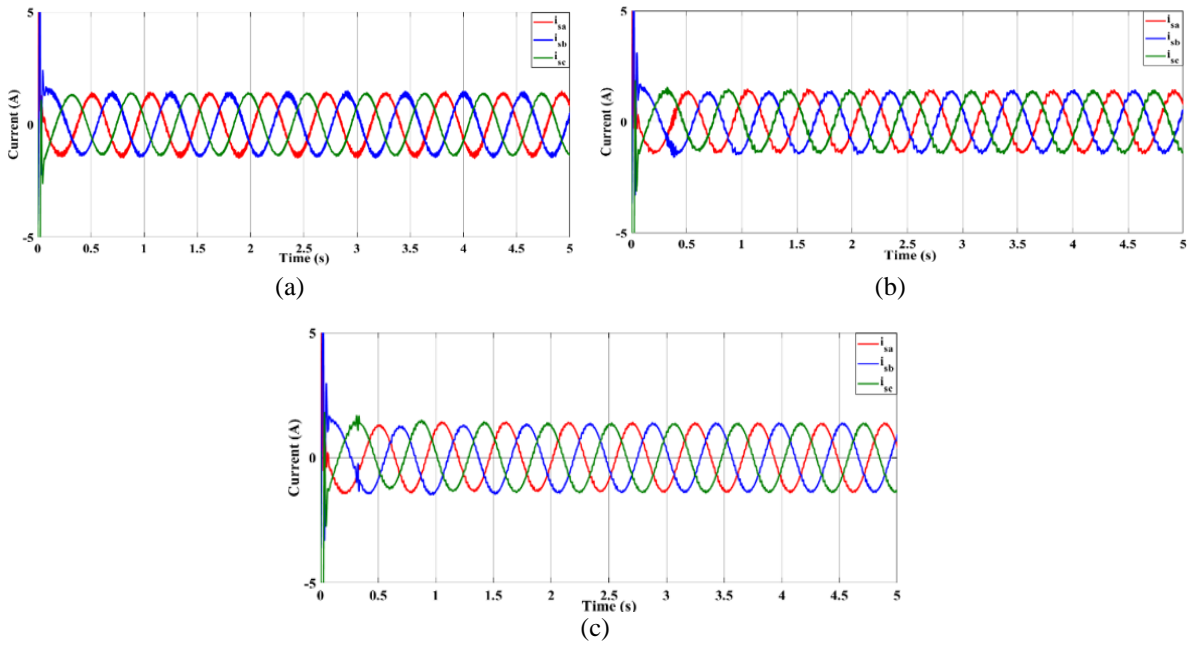


Figure 7. Output current (a) conventional CPS-PWM, (b) modified CPS-PWM, and (c) modified-CPS-PWM with circulating current control

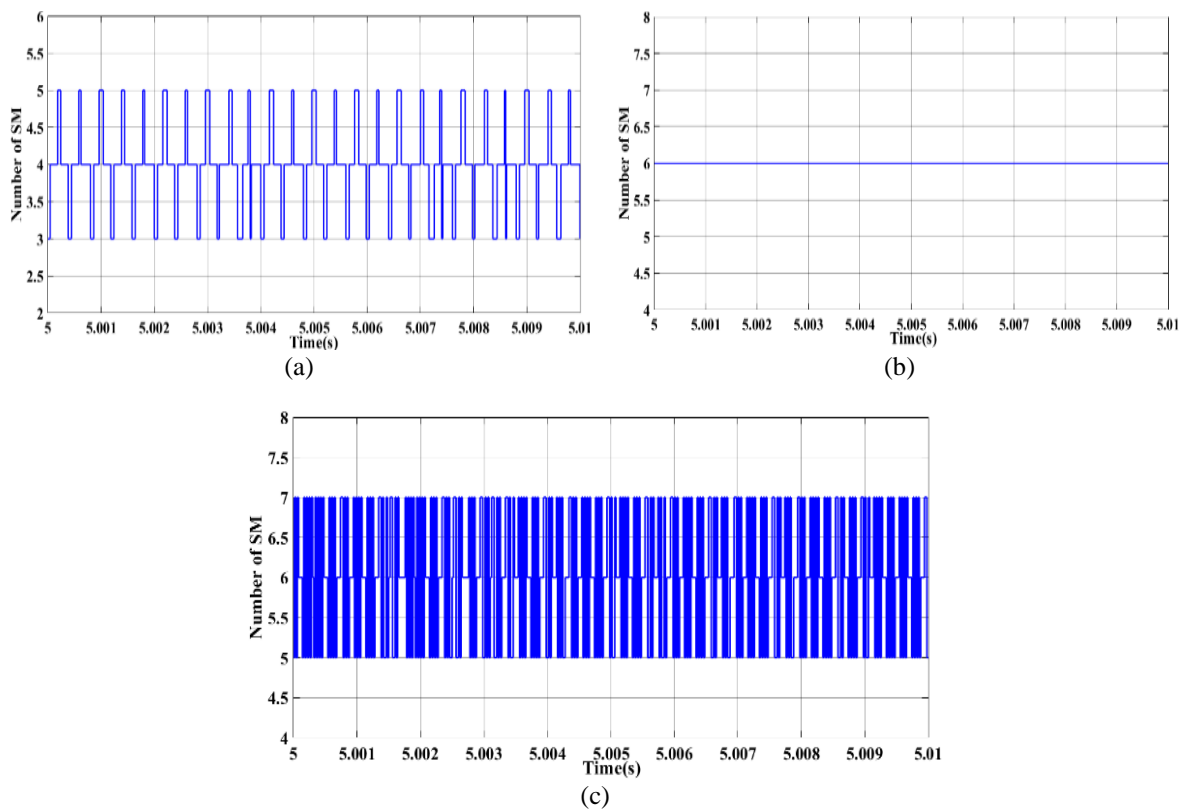


Figure 8. Number of SM in phase a (a) conventional CPS-PWM, (b) modified CPS-PWM, and (c) modified-CPS-PWM with circulating current control

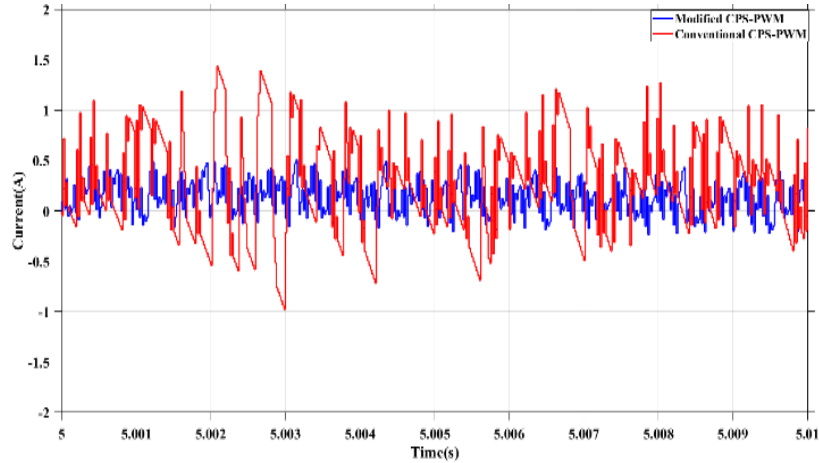


Figure 9. Circulating current

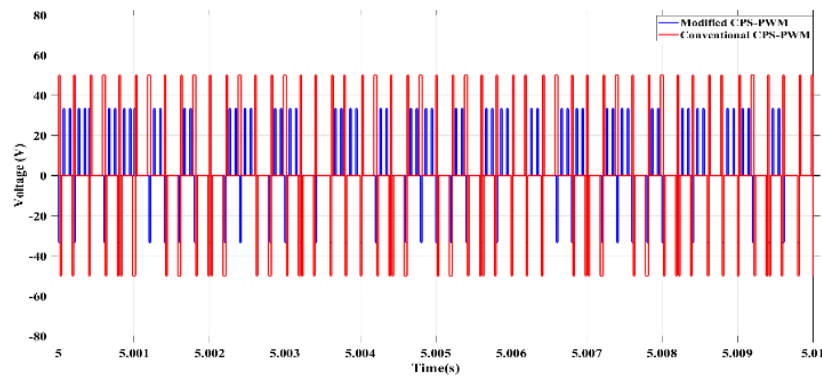


Figure 10. Common mode voltage

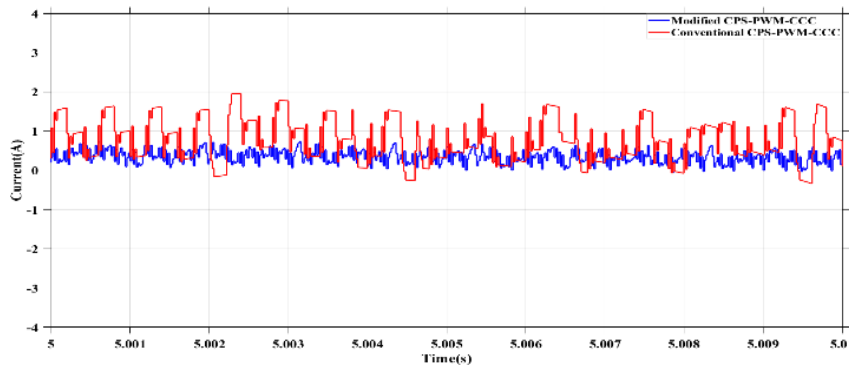


Figure 11. Arm current

#### 4.2. Case 2: Speed=5 Hz (150 rpm)

In this case, the speed of MMC based VSD was increased from 30 rpm to 150 rpm as shown in Figure 12. Due to this increase, the SM capacitors voltage ripples were reduced when the conventional CSP-PWM was used. However, the voltage ripples still exceeded the maximum capacitor voltage limits (157 V) by 12 V approximately as shown in Figure 13(a), the proposed method has reduced the SM capacitor voltage ripples and the maximum voltage ripples were less than the maximum capacitor voltage limit for both cases (with or without circulating current control) as illustrated in Figures 13(b) and 13(c). The output current of the conventional CPS-PWM and the proposed methods are depicted in Figures 14(a), 14(b) and 14(c) respectively. Figures 15(a), 15(b), and 15(c) on the other hand, show the number of inserted SMs for the conventional and the proposed methods.

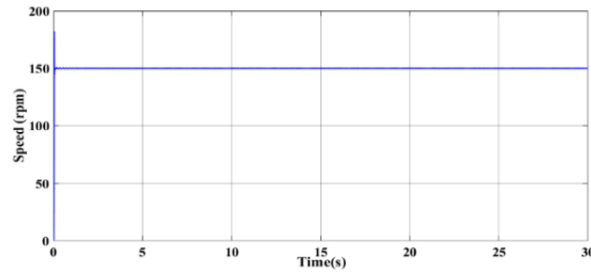


Figure 12. Response of the induction motor to 150 rpm speed

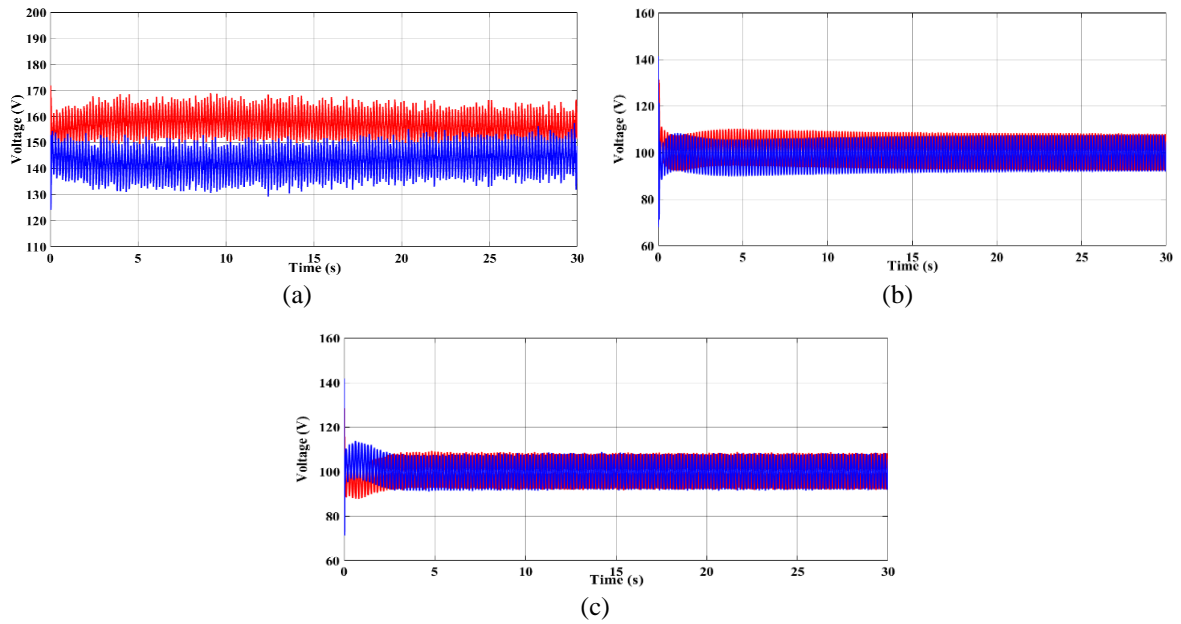


Figure 13. The voltages of SMs capacitors in phase-a (a) conventional CPS-PWM, (b) modified CPS-PWM, and (c) modified-CPS-PWM with circulating current control

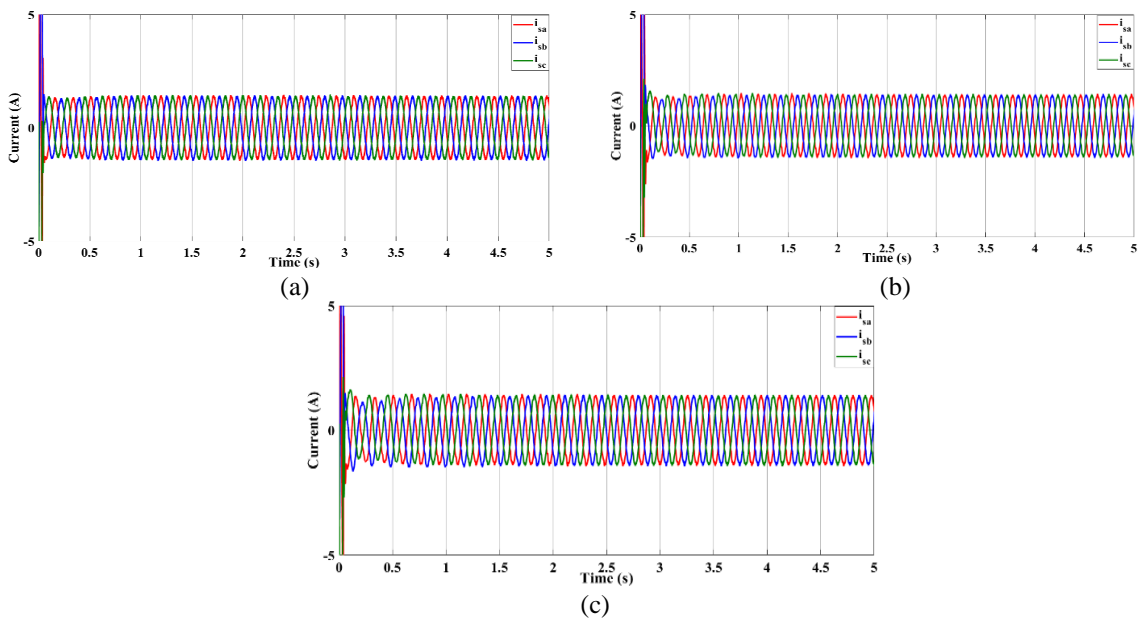


Figure 14. Output current (a) conventional CPS-PWM, (b) modified CPS-PWM, and (c) modified-CPS-PWM with circulating current control

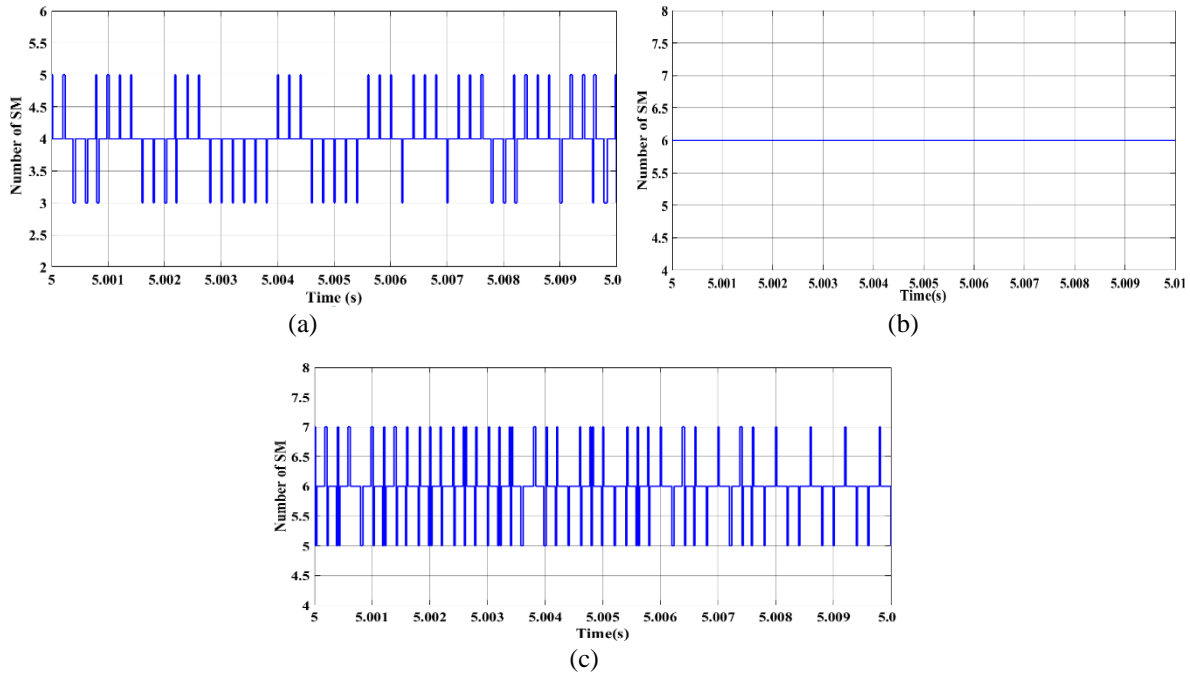


Figure 15. Number of SM in phase a (a) conventional CPS-PWM (b) modified CPS-PWM, and (c) modified- CPS-PWM with circulating current control

**4.3. Case 3: Speed=10 Hz (300 rpm)**

To further investigate the proposed method, we increased the speed to 300 rpm (10 Hz) in Figure 16. By increasing the speed, the SM voltage ripples were reduced significantly as shown in Figure 17. Therefore, it can be concluded that the proposed method is most needed when the speed is less than 10 Hz.

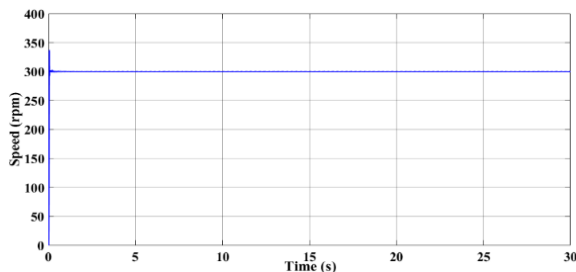


Figure 16. IM response to 300 rpm speed command

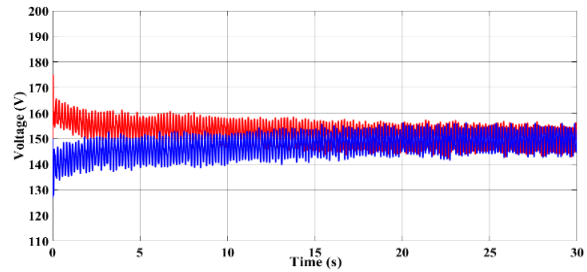


Figure 17. SMs capacitor voltages of phase-a conventional CPS-PWM

**5. CONCLUSION**

The use of MMC in VSD applications has been limited due to large capacitor voltage ripples caused by the low-speed constant torque operations. This paper proposes a method to modify the CPS-PWM to reduce the average voltage of SM Capacitors. By doing so, more ripples can be accommodated without exceeding the maximum SMs capacitor voltage limit. The advantage of the proposed method is that it does not increase the power losses of the MMC and the component ratings remain the same throughout the entire speed range. Simulation results have demonstrated the effectiveness of the proposed method.

**REFERENCES**

[1] J. I. Leon, S. Vazquez, and L. G. Franquelo, "Multilevel Converters: Control and Modulation Techniques for Their Operation and Industrial Applications," in *Proceedings of the IEEE*, vol. 105, no. 11, pp. 2066-2081, Nov. 2017, doi: 10.1109/JPROC.2017.2726583.

- [2] Y. S. Kumar and G. Poddar, "Balanced Submodule Operation of Modular Multilevel Converter-Based Induction Motor Drive for Wide-Speed Range," in *IEEE Transactions on Power Electronics*, vol. 35, no. 4, pp. 3918-3927, April 2020, doi: 10.1109/TPEL.2019.2938096.
- [3] J. Rodriguez, S. Bernet, P. K. Steimer, and I. E. Lizama, "A Survey on Neutral-Point-Clamped Inverters," in *IEEE Transactions on Industrial Electronics*, vol. 57, no. 7, pp. 2219-2230, July 2010, doi: 10.1109/TIE.2009.2032430.
- [4] T. A. Meynard, H. Foch, P. Thomas, J. Courault, R. Jakob, and M. Nahrstaedt, "Multicell converters: basic concepts and industry applications," in *IEEE Transactions on Industrial Electronics*, vol. 49, no. 5, pp. 955-964, Oct. 2002, doi: 10.1109/TIE.2002.803174.
- [5] P. W. Hammond, "A new approach to enhance power quality for medium voltage AC drives," in *IEEE Transactions on Industry Applications*, vol. 33, no. 1, pp. 202-208, Jan.-Feb. 1997, doi: 10.1109/28.567113.
- [6] A. Lesnicar and R. Marquardt, "An innovative modular multilevel converter topology suitable for a wide power range," in *2003 IEEE Bologna Power Tech Conference Proceedings*, 2003, pp. 6 pp. vol. 3, doi: 10.1109/PTC.2003.1304403.
- [7] M. A. Perez, S. Bernet, J. Rodriguez, S. Kouro, and R. Lizana, "Circuit Topologies, Modeling, Control Schemes, and Applications of Modular Multilevel Converters," in *IEEE Transactions on Power Electronics*, vol. 30, no. 1, pp. 4-17, Jan. 2015, doi: 10.1109/TPEL.2014.2310127.
- [8] S. Debnath, J. Qin, B. Bahrani, M. Saedifard and P. Barbosa, "Operation, Control, and Applications of the Modular Multilevel Converter: A Review," in *IEEE Transactions on Power Electronics*, vol. 30, no. 1, pp. 37-53, Jan. 2015, doi: 10.1109/TPEL.2014.2309937.
- [9] A. J. Korn, M. Winkelnkemper, and P. Steimer, "Low output frequency operation of the Modular Multi-Level Converter," in *IEEE Energy Conversion Congress and Exposition*, 2010, pp. 3993-3997, doi: 10.1109/ECCE.2010.5617802.
- [10] R. Picas, J. Pou, S. Ceballos, V. G. Agelidis, and M. Saedifard, "Minimization of the capacitor voltage fluctuations of a modular multilevel converter by circulating current control," in *Annual Conference on IEEE Industrial Electronics Society*, 2012, pp. 4985-4991, doi: 10.1109/IECON.2012.6388984.
- [11] S. P. Engel and R. W. De Doncker, "Control of the Modular Multi-Level Converter for minimized cell capacitance," in *Proceedings of the 2011 14th European Conference on Power Electronics and Applications*, 2011, pp. 1-10.
- [12] R. Picas, J. Pou, S. Ceballos, J. Zaragoza, G. Konstantinou, and V. G. Agelidis, "Optimal injection of harmonics in circulating currents of modular multilevel converters for capacitor voltage ripple minimization," in *IEEE ECCE Asia Downunder*, 2013, pp. 318-324, doi: 10.1109/ECCE-Asia.2013.6579115.
- [13] S. Zhou, B. Li, M. Guan, X. Zhang, Z. Xu, and D. Xu, "Capacitance Reduction of the Hybrid Modular Multilevel Converter by Decreasing Average Capacitor Voltage in Variable-Speed Drives," in *IEEE Transactions on Power Electronics*, vol. 34, no. 2, pp. 1580-1594, Feb. 2019, doi: 10.1109/TPEL.2018.2833503.
- [14] J. Pou, S. Ceballos, G. Konstantinou, G. J. Capella, and V. G. Agelidis, "Control strategy to balance operation of parallel connected legs of modular multilevel converters," in *IEEE International Symposium on Industrial Electronics*, 2013, pp. 1-7, doi: 10.1109/ISIE.2013.6563685.
- [15] M. Vasiladiotis, N. Cherix and A. Rufer, "Accurate Capacitor Voltage Ripple Estimation and Current Control Considerations for Grid-Connected Modular Multilevel Converters," in *IEEE Transactions on Power Electronics*, vol. 29, no. 9, pp. 4568-4579, Sept. 2014, doi: 10.1109/TPEL.2013.2286293.
- [16] M. Winkelnkemper, A. Korn and P. Steimer, "A modular direct converter for transformerless rail interties," in *IEEE International Symposium on Industrial Electronics*, 2010, pp. 562-567, doi: 10.1109/ISIE.2010.5637826.
- [17] A. Antonopoulos, L. Ångquist, S. Norrga, K. Ilves, L. Harnefors, and H. Nee, "Modular Multilevel Converter AC Motor Drives With Constant Torque From Zero to Nominal Speed," in *IEEE Transactions on Industry Applications*, vol. 50, no. 3, pp. 1982-1993, May-June 2014, doi: 10.1109/TIA.2013.2286217.
- [18] S. Sau, S. Karmakar and B. G. Fernandes, "Reduction of capacitor ripple voltage and current in Modular Multilevel Converter based variable speed drives," in *IEEE 3rd International Future Energy Electronics Conference and ECCE Asia (IFEEC 2017 - ECCE Asia)*, 2017, pp. 1451-1456, doi: 10.1109/IFEEC.2017.7992258.
- [19] Y. S. Kumar and G. Poddar, "Medium-Voltage Vector Control Induction Motor Drive at Zero Frequency Using Modular Multilevel Converter," in *IEEE Transactions on Industrial Electronics*, vol. 65, no. 1, pp. 125-132, Jan. 2018, doi: 10.1109/TIE.2017.2721927.
- [20] G. Jia, M. Chen, S. Tang, C. Zhang, and G. Zhu, "Active Power Decoupling for a Modified Modular Multilevel Converter to Decrease Submodule Capacitor Voltage Ripples and Power Losses," in *IEEE Transactions on Power Electronics*, vol. 36, no. 3, pp. 2835-2851, March 2021, doi: 10.1109/TPEL.2020.3016493.
- [21] A. Antonopoulos, L. Ångquist, L. Harnefors and H. Nee, "Optimal Selection of the Average Capacitor Voltage for Variable-Speed Drives With Modular Multilevel Converters," in *IEEE Transactions on Power Electronics*, vol. 30, no. 1, pp. 227-234, Jan. 2015, doi: 10.1109/TPEL.2014.2316273.
- [22] G. Konstantinou, J. Pou, S. Ceballos, R. Picas, J. Zaragoza and V. G. Agelidis, "Control of Circulating Currents in Modular Multilevel Converters Through Redundant Voltage Levels," in *IEEE Transactions on Power Electronics*, vol. 31, no. 11, pp. 7761-7769, Nov. 2016, doi: 10.1109/TPEL.2015.2512842.
- [23] S. B. Bashir and A. R. Beig, "An improved voltage balancing algorithm for grid connected MMC for medium voltage energy conversion," *International Journal of Electrical Power and Energy Systems*, vol. 95, pp. 550-560, 2018. doi: 10.1016/j.ijepes.2017.09.002.
- [24] Bashir, Safia Babikir, Hasan A. Zidan, and Zulfqar Ali Memon. "Power balancing of grid connected PV system based on MMC under different irradiation conditions," *International Journal of Electrical Power and Energy Systems*, vol. 117, 2020, doi: 10.1016/j.ijepes.2019.105717.
- [25] H. A. Zidan and S. B. Bashir. "Sensor-less vector control of induction motor at low-speed operation using modular multilevel converter," *Australian Journal of Electrical and Electronics Engineering*, vol. 16, no. 3, pp. 127-135, 2019, doi: 10.1080/1448837X.2019.1626528.

**BIOGRAPHIES OF AUTHORS**

**Safia Babikir Bashir**     received her B.Sc. degree in electrical engineering from Ajman University, UAE, in 2013 and her MSc degree in electrical engineering from The Petroleum Institute, UAE, in 2016. Currently, she works as a research assistant in the Smart Grid and Power Systems research group at the University of Sharjah. Her research interest includes Multilevel converters, electric drive, renewable energy system, and HVDC transmission systems. She can be contacted at email: safia.mohamed@sharjah.ac.ae.



**Hasan Abdel Rahim A. Zidan**     received his B.Sc. degree in electrical engineering from AMTA, Alexandria, in 1991, and his MSc and Ph.D. degrees in control engineering from Kyushu Institute of Technology (KIT), JAPAN, in 1998,2001. Currently, he is working as an Associate Professor in the electrical and computer engineering department at Ajman University. His research interest includes Fuzzy and Neural Network applications, machine control, electric drive, and renewable energy system. He can be contacted at email: h.alhaj@ajman.ac.ae.



**Zulfiqar Ail Memon**     received his B.Eng. degree in electrical engineering from MUET, Jamshoro Pakistan, in 1986 and his Ph.D. degrees in Automation and Robotics from Brunel University London, UK, in 1991. Currently, he is working as an Assistant Professor in the electrical and computer engineering department at Ajman University. His research interest includes electric drive, smart grid, and renewable energy systems. He can be contacted at email: z.memon@ajman.ac.ae.